Heterogeneous Catalysis

DOI: 10.1002/ange.201107625

Structural Requirements in Lithium Cobalt Oxides for the Catalytic Oxidation of Water**

Graeme P. Gardner, Yong Bok Go, David M. Robinson, Paul F. Smith, Joke Hadermann, Artem Abakumov, Martha Greenblatt, and G. Charles Dismukes**

The development of water oxidation catalysts (WOCs) to replace costly noble metals in commercial electrolyzers and solar fuel cells is an unmet need that is preventing the global development of hydrogen fuel technologies. Two of the main challenges in realizing catalytic water splitting are lowering the substantial overpotential that is required to achieve practical operating current densities in the O_2-evolving half-reaction at the anode, and the use of earth-abundant elements for the fabrication of inexpensive electrodes that are free from noble metals. To meet these challenges, molecular catalysts that are based upon the cubic $CaMn_4O_x$ core within photosystem II in photosynthetic organisms, which is the gold standard of catalytic efficiency, have begun to appear.[1–3]

Among solid-state materials, several noble-metal oxides, which include IrO_2 and RuO_2, are already in use in industrial electrolyzers, but are not globally scalable.[4–6] Aqueous solutions of cobalt phosphate form water-oxidation catalysts under electrolysis[7,8,10] and photolysis[9] that are suitable for the fabrication of noncrystalline electrode materials. Nanocrystalline spinel-phase metal oxides (AM_2O_4, M = transition metals) that are comprised of M_4O_4 cubical subunits and are active water oxidation catalysts have been developed.[11,12] The catalytic activity of the spinel Co_3O_4 has been reported for Co_3O_4 nanorods that are incorporated into SBA-15 silica,[12] as well as Co_3O_4 nanoparticles that are adsorbed onto Ni electrodes.[13] $NiCo_2O_4$ spinel also oxidizes water when the nanoparticles are electrophoretically deposited onto a Ni electrode.[14] Reports that examined the effect of lithium doping on the surface of Co_3O_4 electrodes in solutions of KOH attributed the higher evolution rate of O_2 to better electrical conductivity.[15,16] However, the oxidation of water by Co_3O_4 was strongly dependent on crystallite size and surface area and frequently necessitates high overpotentials and alkaline conditions to accelerate the rate of reaction.[14,17]

In contrast, we recently reported that the catalytically inert spinel $LiMn_2O_4$ gives spinel λ-MnO_2, which is an active water oxidation catalyst, upon topotactic delithiation. Thus, the importance of removing the A-site lithium for catalysis by the cubic Mn_4O_4 core of spinels was revealed.[11]

Metal oxides that contain lithium are well-researched cathode materials for lithium-ion batteries. In particular, lithium cobalt oxide has been implemented extensively for this application, and its electrochemical properties have been examined thoroughly. Lithium cobalt oxide occurs as two crystalline polymorphs of identical composition (Figure 1):

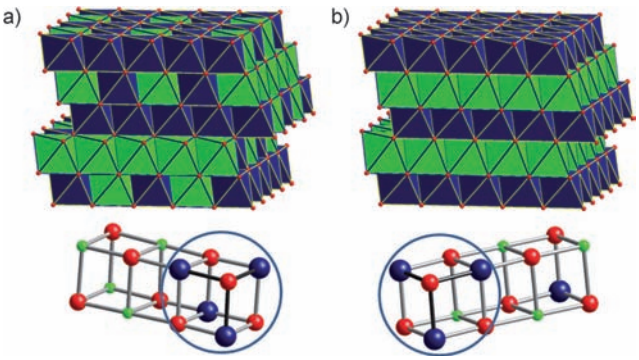

Figure 1. Polyhedral and ball-and-stick models of a) Cubic $Li_2Co_2O_4$ with a Co_4O_4 core, analogous to that of the molecular cubane catalysts,[1] and b) Layered $LiCoO_2$ with alternating metal layers without Co_4O_4 cubes. All metal centers are octahedrally coordinated. Li, Co, and O atoms are shown as green, blue, and red, respectively.

cubic spinel-like $Li_{1+y}Co_2O_4$ ($Fd\bar{3}m$; $y = 1$ or less), simplified as $Li_2Co_2O_4$ and rhombohedral layered $LiCoO_2$.[18,19] Layered lithium cobalt oxide is an effective cathode material for lithium-ion batteries as it has a higher energy density and better stability than the corresponding cubic phase.[20] Herein, we show that of the two, only the cubic phase $Li_2Co_2O_4$ is active in catalyzing the oxidation of water, when driven either electrolytically or by a photochemically generated oxidant.

We investigated lithium cobalt oxides to test the bio-inspired hypothesis,[21] namely, whether the cubic M_4O_4 core is a general feature for efficient catalysis of water oxidation.[11] Comparison of the atomic structures of cubic $Li_2Co_2O_4$ and layered $LiCoO_2$ (Figures 1a and b, respectively) reveals that

[*] G. P. Gardner, Dr. Y. B. Go, D. M. Robinson, P. F. Smith, Prof. M. Greenblatt, Prof. G. C. Dismukes
Department of Chemistry and Chemical Biology Rutgers
The State University of New Jersey
Piscataway, NJ 08854 (USA)
E-mail: martha@rutchem.rutgers.edu
dismukes@rci.rutgers.edu
Prof. J. Hadermann, Prof. A. Abakumov
Electron Microscopy for Materials Research
Physics Department, University of Antwerp
Groenenborgelaan, 171B-2020, Antwerp (Belgium)

[**] This work was supported by Rutgers University, AFOSR-FA9550-05-1 and FA9550-11-1 (G.C.D.). We acknowledge partial support by NSF-DMR-0966829 (M.G. and Y.B.G.) and an NSF predoctoral fellowship (D.M.R.). We thank Paul Field for help with elemental analysis, Zhijuan Zhang for BET measurements, and Jun Chen and Gerry Swiegers for help with electrochemical measurements. This paper honors the memory of our teacher, Peter Gabriel.

Supporting information for this article is available on the WWW under http://dx.doi.org/10.1002/anie.201107625.

only the cubic $Li_2Co_2O_4$ possesses cubic Co_4O_4 units within the lattice, whereas the layered $LiCoO_2$ is comprised of alternating layers of Co–O and Li–O octahedra that form $LiCo_3O_4$ units and not cubic Co_4O_4 subunits.

A previously described sol-gel method[22] was adapted to prepare nanocrystalline powders of cubic $Li_2Co_2O_4$ and layered $LiCoO_2$. An aqueous solution of $LiNO_3$, $Co(NO_3)_2{\cdot}6H_2O$, citric acid, and urea was evaporated at 80 °C for 4–6 h. The precursor powder was then decomposed at different temperatures (400, 500, 600, and 700 °C) for 1–2 h. The products were characterized by powder X-ray diffraction (PXRD), precession electron diffraction (PED), scanning electron microscopy (SEM), BET surface area analysis, thermogravimetric analysis (TGA), and differential scanning calorimetry (DSC). The composition of the products was analyzed by inductively coupled plasma optical emission spectrometry (ICP-OES).

The PXRD patterns in Figures 2 a–d show a structural transformation upon increasing the temperature of the synthesis, from cubic at 400 °C to the thermodynamically favored layered phase above 600 °C. A mixture of these two phases appears at 500 °C. The splitting of peaks 222 and 440, as well as the shift of the 111 peak, indicate the formation of layered $LiCoO_2$.[23,24] Co_3O_4 was not detected at any temperature. Heating can be accompanied by a substantial increase in crystallinity and particle size when the samples are synthesized by solid-state reactions. The average particle size of the layered 800-$LiCoO_2$ that was prepared by a solid-state reaction was 1–2 μm and yielded sharper PXRD reflections (Figures S1 and S2 in the Supporting Information). In contrast, the crystallite size was limited to nanometer dimensions with sol-gel synthesis. SEM images of the products reveal average particle sizes of 50 nm for the materials that were synthesized at low temperatures (Figures 3 a–c) and 100 nm for the material that was synthesized at the highest temperature (Figure 3 d). BET measurements of the material that was produced at 400 °C in the sol-gel (56.19 m^2g^{-1}) show that the surface area is four times that of the material that was synthesized at 700 °C (Table S1 in the Supporting Information), which is consistent with the doubling of particle size, as shown by SEM (Figure 3). The lithium/cobalt ratios (1:1 by ICP-OES) were independent of the synthesis temperature for all of the samples (Table S1 in the Supporting Information).

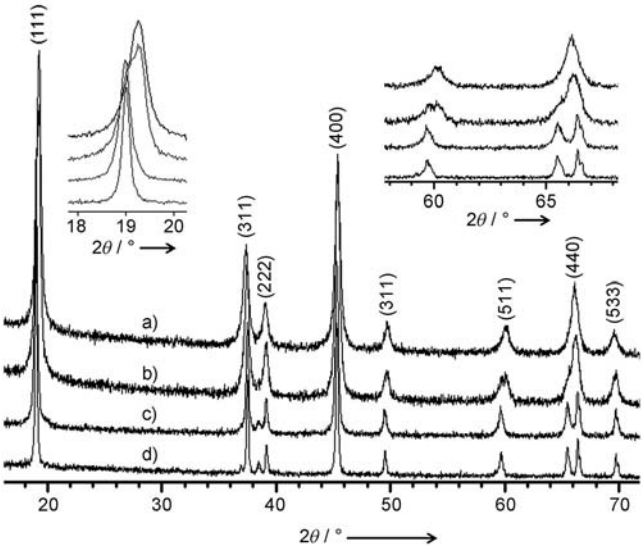

Figure 2. Powder XRD patterns of lithium cobalt oxide calcined at a) 400 °C, b) 500 °C, c) 600 °C, and d) 700 °C, respectively. Insets show the phase transformation from cubic to layered with increasing calcination temperature.

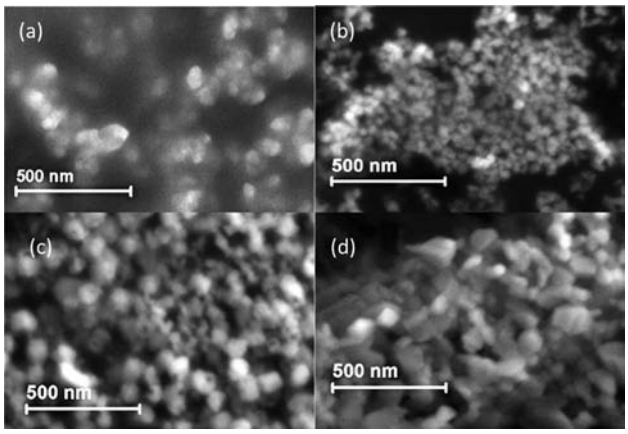

Figure 3. SEM images of lithium cobalt oxides calcined at a) 400 °C, b) 500 °C, c) 600 °C, and d) 700 °C.

Analyses of the sol-gel precursor by TGA and DSC were conducted in parallel to continuously detect mass loss and the heat capacity during the synthesis of the product. The TGA and DSC curves shown in Figure 4 indicate two mass losses,

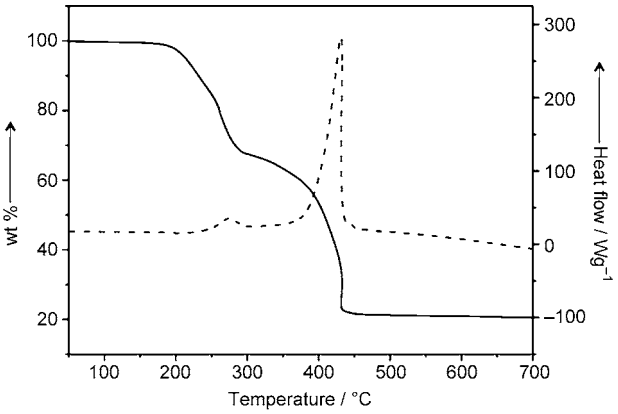

Figure 4. TGA (solid line) and DSC analyses (dashed line) of the sol-gel precursor dried at 130 °C for 12 h.

which correspond to the decomposition of ammonium citrate and ammonium nitrate between 200 °C and 300 °C, and the decomposition of remaining LiCo(citrate) to $Li_2Co_2O_4$ between 300 °C and 430 °C.[24] Between 430 °C and 700 °C there is no further mass loss and only a slow conversion to the more stable layered $LiCoO_2$. These data demonstrate that there are no residual organic compounds or water present above 430 °C.

The photocatalytic oxidation of water was monitored in solution through the detection of dissolved O_2 by using a Clarke-type electrode equipped with a thermostat. The potential that was needed to drive the oxidation of water was provided by a commonly used photosensitizer assay ($[Ru(bpy)_3]^{2+}/Na_2S_2O_8$, bpy = 2,2-bipyridine) in a sodium hexafluorosilicate buffer[5], adjusted with $NaHCO_3$ to pH 5.8.[3,11] The evolution of O_2 that was driven by visible light was normalized to the total number of moles of cobalt in solution and to the surface area of the catalyst (Figure 5, top and bottom, respectively). The amount of O_2 that was evolved was independently determined by GC analysis of the solution headspace (for details, see the Supporting Information).

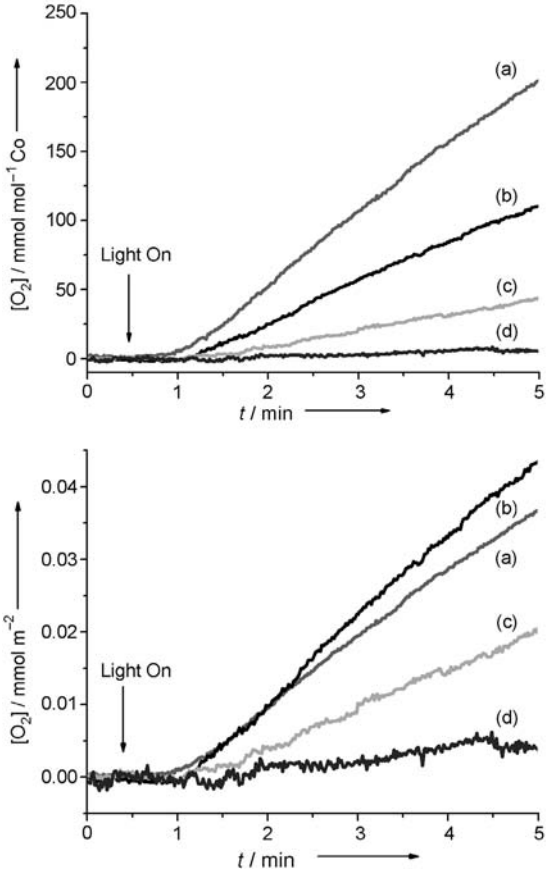

Figure 5. Concentration of dissolved O_2 as measured by using a Clark-type electrode at 23 °C, pH 5.8 for lithium cobalt oxides synthesized at a) 400 °C, b) 500 °C, c) 600 °C, and d) 700 °C, normalized to total moles of cobalt (top graph), and total surface area of the catalyst (bottom graph). Illumination begins after a lag time of 20 s. Conditions: $[Ru(bpy)_3]^{2+}$ (1 mM), $Na_2S_2O_8$ (20 mM), and catalyst (200 ppm) at pH 5.8.

The catalyst turnover frequency (TOF) was $1.0 \times 10^{-3}\ s^{-1}$ for pure cubic 400-$Li_2Co_2O_4$ per bulk cobalt atom, which was determined from the initial slope of the dissolved O_2 concentration (Figure 5, top). This value is 10-fold greater than for λ-MnO_2 that was prepared from the analogous $LiMn_2O_4$ spinel.[11] However, as only surfaces sites are known to be active in catalysis,[12,13] this rate is considered a conservative, lower-boundary estimate. When normalized to the amount of surface-accessible cobalt (calculated from the BET surface area and crystal lattice parameters), the TOF is $1.9 \times 10^{-2}\ s^{-1}$. The catalytic activity per unit of surface area decreases with increasing calcination temperature and the corresponding change in the crystal structure (Figures 5a–c). Pure layered $LiCoO_2$ is not catalytically active (Figure 5d). Although the material that was synthesized at 600 °C is primarily layered (based on the PXRD pattern, Figure 2c), the presence of some residual cubic phase was established by PED (for details, see the Supporting Information). Hence, we conclude that the small amount of cubic $Li_2Co_2O_4$ that is present in the 600 °C material is likely to be responsible for the residual evolution of O_2 (Figure 5c).

The structural and chemical integrity of cubic $Li_2Co_2O_4$ before and after photocatalysis was monitored by PXRD and ICP-OES, and demonstrated no change in the crystal structure (Figure S3 in the Supporting Information), as well as the absence of dissolution of cobalt in sample washes (less than 0.1% dissolved cobalt in materials synthesized at low- and high-temperatures).

Electrochemical measurements were performed on membrane electrode assemblies (MEA) in a 3-electrode configuration (for details, see the Supporting Information). MEAs were prepared by spin-coating indium–tin oxide (ITO) electrodes with a controlled amount of a suspension of neutralized Nafion (in MeOH, 4% by weight) and lithium cobalt oxide powders.[25] Bulk electrolysis was performed at 1.2 V versus a Ag/AgCl reference electrode in a phosphate buffer at pH 7.2 and provided clear evidence that the MEA that contains cubic 400-$Li_2Co_2O_4$ has a 50-fold greater current density (greater than $250\ \mu A\ cm^{-2}$), which results from the oxidation of water, than the MEA that contains layered 700-$LiCoO_2$ with an equal loading ($< 10\ \mu A\ cm^{-2}$, Figure 6). The 700-$LiCoO_2$ is only slightly above the background current (for MEA with Nafion only). The consistent trend in catalytic turnover in the results from both the solution assay (Figures 5a–d) and the electrolytic MEAs (Figure 6), establishes unequivocally that the crystal structure of lithium cobalt

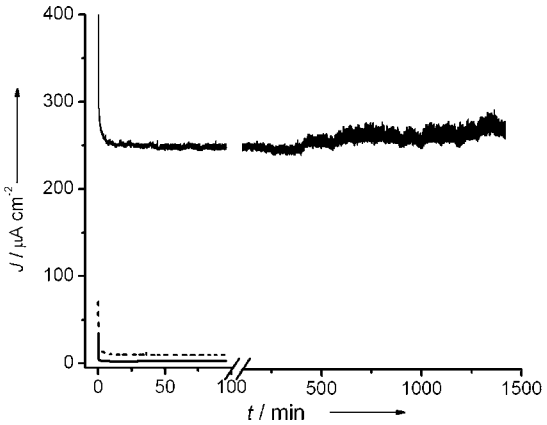

Figure 6. Bulk electrolysis on ITO MEAs prepared with Nafion/catalyst films of 400-$Li_2Co_2O_4$ (solid black line), 700-$LiCoO_2$ (dashed gray line), and the Nafion-only control (solid gray line). Conditions: 1.2 V versus Ag/AgCl, pH 7.2, phosphate buffer (0.1 M).

oxides determines their catalytic activity, and that the M_4O_4 cubical core provides a major advantage for the oxidation of water.

Previously, the electrolysis of water was demonstrated to be dependent on the surface area of a Co_3O_4 nanospinel catalyst (with A = Co not Li) that was loaded onto Ni foam electrode. In this case, smaller particles gave a higher catalytic activity.[12] In the photochemical and electrochemical systems in this study, a decrease in the surface area clearly decreases the activity of the catalyst. A similar dependence was recorded for λ-MnO_2.[11] In contrast, neither surface area nor particle size was found to activate the catalytic oxidation of water by the layered polymorph $LiCoO_2$.

With identical stoichiometries and coordination numbers for all metal centers in the two polymorphs of lithium cobalt oxide, a comparison was made and the atomic arrangement was identified as the major determinant of the catalytic activity. The bioinspired hypothesis that was tested in this study[21] posits that the oxometallic M_4O_4 cubes of cobalt that are present in cubic $Li_2Co_2O_4$ may function analogously to the $CaMn_4O_x$ core of the photosynthetic WOC, and to the previously described molecular cubane catalysts made from manganese[1] and cobalt.[3] As of yet, there is no direct evidence that identifies exactly what is responsible for the activity of cubic oxometallic cores in the oxidation of water in any of these systems. Although the nanocrystalline component is a significant factor in eliciting a higher catalytic activity in heterogeneous catalysis, it is not singularly, nor primarily responsible in the case of lithium cobalt oxides. Given the high natural abundance, ease of synthesis, high thermal and redox cycling stability, intrinsic high TOF, and stable current density of cubic $Li_2Co_2O_4$, this material is promising for applications in electrolyzers and solar-driven fuel cells.

Received: October 28, 2011
Revised: December 19, 2011
Published online: January 11, 2012

Keywords: cobalt · heterogeneous catalysis · lithium · spinels · water splitting

[1] R. Brimblecombe, A. Koo, G. C. Dismukes, G. F. Swiegers, L. Spiccia, *J. Am. Chem. Soc.* **2010**, *132*, 2892 – 2894.
[2] M. M. Najafpour, T. Ehrenberg, M. Wiechen, P. Kurz, *Angew. Chem.* **2010**, *122*, 2281 – 2285; *Angew. Chem. Int. Ed.* **2010**, *49*, 2233 – 2237.
[3] N. S. McCool, D. M. Robinson, J. E. Sheats, G. C. Dismukes, *J. Am. Chem. Soc.* **2011**, *133*, 11446 – 11449.
[4] M. Hara, C. C. Waraksa, J. T. Lean, B. A. Lewis, T. E. Mallouk, *J. Phys. Chem. A* **2000**, *104*, 5275 – 5280.
[5] N. D. Morris, M. Suzuki, T. E. Mallouk, *J. Phys. Chem. A* **2004**, *108*, 9115 – 9119.
[6] A. T. Marshall, R. G. Haverkamp, *Electrochim. Acta* **2010**, *55*, 1978 – 1984.
[7] M. W. Kanan, D. G. Nocera, *Science* **2008**, *321*, 1072 – 1075.
[8] S. E. S. El Wakkad, A. Hickling, *Trans. Faraday Soc.* **1950**, *46*, 820 – 824.
[9] B. S. Brunschwig, M. H. Chou, C. Creutz, P. Ghosh, N. Sutin, *J. Am. Chem. Soc.* **1983**, *105*, 4832 – 4833.
[10] O. Suzuki, M. Takahashi, T. Fukunaga, J. Kuboyama, US Patent, 3,399,966, **1968**.
[11] D. M. Robinson, Y. B. Go, M. Greenblatt, G. C. Dismukes, *J. Am. Chem. Soc.* **2010**, *132*, 11467 – 11469.
[12] F. Jiao, H. Frei, *Energy Environ. Sci.* **2010**, *3*, 1018 – 1027.
[13] A. J. Esswein, M. J. McMurdo, P. N. Ross, A. T. Bell, T. D. Tilley, *J. Phys. Chem. C* **2009**, *113*, 15068 – 15072.
[14] J. Yang, J. Li, H. Lin, X. Yang, X. Tong, G. Guo, *J. Appl. Electrochem.* **2006**, *36*, 945 – 950.
[15] P. Rasiyah, A. C. C. Tseung, *J. Electrochem. Soc.* **1983**, *130*, 365 – 368.
[16] P. Rasiyah, A. C. S. Tseung, *J. Electrochem. Soc.* **1984**, *131*, 803 – 808.
[17] N. K. Singh, J. P. Singh, R. N. Singh, *Int. J. Hydrogen Energy* **2002**, *27*, 895 – 903.
[18] Y. Shao-Horn, S. A. Hackney, C. S. Johnson, A. J. Kahaian, M. M. Thackeray, *J. Solid State Chem.* **1998**, *140*, 116 – 127.
[19] Y. Shao-Horn, S. A. Hackney, A. J. Kahaian, M. M. Thackeray, *J. Solid State Chem.* **2002**, *168*, 60 – 68.
[20] H. Gabrisch, R. Yazami, B. Fultz, *J. Electrochem. Soc.* **2004**, *151*, A891 – A897.
[21] G. C. Dismukes, R. Brimblecombe, G. A. N. Felton, R. S. Pryadun, J. E. Sheats, L. Spiccia, G. F. Swiegers, *Acc. Chem. Res.* **2009**, *42*, 1935 – 1943.
[22] S. Vivekanandhan, M. Venkateswarlu, N. Satyanarayana, *J. Alloys Compd.* **2007**, *441*, 284 – 290.
[23] S. Choi, A. Manthiram, *J. Solid State Chem.* **2002**, *164*, 332 – 338.
[24] B. Garcia, P. Barboux, F. Ribot, A. Kahn-Harari, L. Mazerolles, N. Baffier, *Solid State Ionics* **1995**, *80*, 111 – 118.
[25] J. Suntivich, H. A. Gasteiger, N. Yabuuchi, Y. Shao-Horn, *J. Electrochem. Soc.* **2010**, *157*, B1263 – B1268.

